Macromolecules
ARTICLE

Macromolecules **2009**, *42*, 7969–7973 **7969**
DOI: 10.1021/ma9013109

Interdiffusion of Short Chain Oligomers into an Entangled Polymer Film

Flint Pierce,*,† Dvora Perahia,† and Gary S. Grest‡

†*Department of Chemistry, Clemson University, Clemson, South Carolina 29634, and*
‡*Sandia National Laboratories, Albuquerque, New Mexico 87185*

Received June 17, 2009; Revised Manuscript Received September 3, 2009

ABSTRACT: The crossover from a simple liquid to an unentangled oligomer diffusing into liquid and glassy entangled polymer matrices is studied by molecular dynamics simulations. The oligomer film is described by a bead−spring model of chain length $N_o = 10$ and 50 while the polymer matrix consist of chains of length $N_p = 500$. Results are compared to interdiffusion into an unentangled polymer matrix of chain length $N_p = 50$. Diffusion of the oligomer into the polymer is observed in all cases as evidenced by $t^{1/2}$ scaling of both the mass uptake of the oligomer by the polymer and oligomer density profiles on the polymer-rich side of the interface as a function of time t. On the oligomer-rich side, the scaling exponent is less than 1/2 due to the swelling of the polymer film and depends on the chain length of both the oligomer and polymer. Oligomer diffusivities into the entangled polymer matrix are highly concentration dependent, in contrast to a nearly constant diffusivity for penetration into the unentangled polymer. The roughness of the polymer film evolves as $t^{0.2}$ for both liquid and glassy films.

I. Introduction

Polymeric interfaces are used in a variety of applications from thin surface layers in coatings and adhesives to interfacial regions in clean energy devices such as fuel cells and polymer photovoltaics.[1−3] Of particular interest are interfaces between different polymers that render composites with complex tunable properties. The simplest example where the macroscopic dynamics of interdiffusion plays a critical role is manifested in self-healing of defects.[4]

Understanding interdiffusion of polymer molecules into polymeric matrices presents several challenges arising from the large range of time scales that govern the process. The dynamics depends on molecular parameters including the chemical nature and the sizes of the components that reside at the interface and the initial dynamics as reflected in the temperature with respect to their glass transition temperatures, T_g. As mass transport takes place, interdiffusion is also coupled to macroscopic changes in the polymer film including swelling as well as phase changes such as gel formation and dissolution. When local dynamics including chain re-engagements, reptation motion, and disentanglements are of the order of magnitude of the mass transport at the interface, deviation from a classical Fickian diffusive process for intermediate times is expected.

The technological significance of interdiffusion has driven a large number of experimental[5−16] and theoretical[12,17−23] studies. Some of the these studies investigated interdiffusion of short oligomers below the entanglement length N_e.[20,21] Other studies have focused on interdiffusion for two entangled polymers, for which both are much longer than the entanglement length N_e.[5,6,9,11,12,17−19,22,23] Kramer et al. followed the diffusion of Au nanoparticles markers which were initially placed at the interface between two monodispersed entangled polystyrene (PS) films.[5] They found that the displacement of the markers scaled with time t as $t^{1/2}$, in agreement with Fickian diffusion. Reiter et al. extended this work to include diffusion of Au nanoparticle markers at the interface between PS films of different molecular weight, finding a weight-dependent induction time for the movement of the markers in addition to their eventual Fickian diffusion.[10] Other studies have used nuclear reaction analysis to study the interdiffusion of protonated and deuterated PS films.[7,9] Since the Flory−Huggins interaction parameter, χ, between protonated and deuterated segments is nonzero, the interfacial width was found to increase as t^{α} with α between 0.27 and 0.36 depending on temperature for early times and then saturate for late times. Short oligomers interdiffusing into an entangled polymer have been studied by Bucknall et al.[13] using neutron reflectivity. These studies demonstrate the complexity of interdiffusion process where small changes in local interactions and dynamics strongly affect the process.

The interdiffusion of polymers is often governed by the degree of their entanglements. With solvents that vary from simple liquids on one end to highly entangled macromolecules on the other, the current study investigates interdiffusion in the crossover region between these two extremes. The mass uptake by polymers is often characterized by t^{α} where t is time.[14,24,25] Fickian diffusion, which is often referred to as class I diffusion, occurs for the interdiffusion of two simple liquids. The process is characterized by $\alpha = 1/2$ for the mass uptake. Diffusion into liquid, nonentangled polymers, where the matrix is viewed as a elastic solid, also follows the Fickian form of the diffusion. For two entangled polymers, the mass uptake is expected to scale as $t^{1/2}$ only for times longer than the disentanglement time $\tau_d \propto N^3$. Class II diffusion is defined for penetration into a glassy polymer film, where material misfits induced in the film[26] result in a constant velocity solvent concentration front[26−28] proceeded by a Fickian precursor foot.[24,29−31] Anomalous diffusion is observed when a penetrant diffuses through a medium containing either static obstacles or for solvent that diffuses by hopping after a characteristic delay time, possibly as a result of site binding.[32−34] For anomalous diffusion, as is the case for diffusion through cellular membranes, the mean-square displacement of penetrant follows a power law less than 1.

Prior experimental and theoretical studies have demonstrated the need for a comprehensive approach that encapsulates the time and length scales relevant to interdiffusion in polymeric interfaces while controlling the polymer−polymer interactions.

*Corresponding author. E-mail: fpierce@sandia.gov.

Published on Web 09/25/2009

One technique to study the relevant time and length scales for interdiffusion is molecular dynamics (MD) simulations, though modeling the interdiffusion of two entangled polymers still presents formidable challenges. The simplest end of this complex challenge has been studied by Tsige and Grest,[35,36] who investigated the penetration of spherical monomeric solvents into liquid and glassy polymer films. In this region they found that the process is dominated by Fickian type diffusion. The current study enhances the complexity to investigate the crossover from a simple liquid of spherical monomers to unentangled oligomers below or near the polymer entanglement length. This crossover is the first necessary step in developing a comprehensive understanding of the interdiffusion where entanglements dominate.

Another important parameter that can influence the interdiffusion is the shape of the penetrant molecule. This has been demonstrated by studies of diffusion of small organic molecules into polymeric matrices. Kwan et al. studied interdiffusion of a homologous series of linear alkanes[14] and esters[15] with a polyamide matrix, noting the importance of solvent size and shape on the process of diffusion into the polymer layer and observing Fickian diffusion in a temperature range from 23 to 85 °C. von Meerwall et al.,[37] in a study of the diffusion of a wide variety of plasticizers in PVC, showed that the diffusion of small molecule solvents is primarily along their long axis, both in polymer matrices and in their own neat melts. Such curvilinear motion for the diffusion of linear molecules is to be expected due to the reduced requirements for rearrangement of the polymer matrix to accommodate the diffusing solvent molecule. The diffusion of oligomers into a polymer matrix may exhibit important differences to the interdiffusion of monomer solvents and polymer films. This study also probes shape and size effects for solvents by extension of a spherical monomer to an elongated oligomer.

This work focuses on the crossover from the interdiffusion of small penetrants and monomer solvents with a polymer film and studies of the interdiffusion and welding of two entangled polymer films. We investigate interdiffusion between oligomer films and entangled polymer films both above and below the glass transition temperature through molecular dynamics simulations. In section II, we present details of the simulation method. In section III results for the density profiles and mass uptake of the oligomer by the polymer film as a function of time, the density dependence of the diffusivities of the oligomer chains, and the evolution of the roughness of the polymer surfaces are presented. Section IV concludes with a brief summary and discussion of these results.

II. Simulation Method

In this study we follow the interdiffusion of polymer and oligomer thick films, placed in close contact at $t = 0$. Films are composed of bead−spring chains of Lennard-Jones monomers of diameter σ which vary in thickness from 70σ to 100σ, depending on the chain length. The simulation box is periodic in x and y with fixed boundaries in z. The film−film interface is parallel to the $x-y$ plane, diffusion fronts proceeding along the z-direction. The box dimensions are $L_x = 720\sigma$ and $L_y = 40\sigma$. The upper oligomer film consists of $M_o = 163\,209$ chains of length $N_o = 10$ or $M_o = 48\,000$ chains of length $N_o = 50$, while $M_p = 4800$ chains of length $N_p = 500$ comprise the lower polymer film. One simulation with $M_o = 2\,400\,000$ monomer solvent was also done. For comparison, we also simulated a system of $N_o = 10$ chains interdiffusing into a matrix of chain length $N_p = 50$. For all simulations, the upper surface of the oligomer is far from the upper bounding wall and forms a liquid/vapor interface. In this way the pressure is maintained at $P = 0$. Upon initiation, the upper and lower films are placed as close together as possible without overlap. Because of the finite roughness of the polymer surface, a small gap of approximately 3σ is present between the two films at the beginning of the simulation. In all cases, this gap closes within a few thousand time steps.

Monomers within and between chains interact via a standard Lennard-Jones potential with a cutoff of $r_c = 2.5\sigma$.

$$U(r_{ij}) = 4\varepsilon_{ij}\left[\left(\frac{\sigma}{r_{ij}}\right)^{12} - \left(\frac{\sigma}{r_{ij}}\right)^{6}\right] \quad (1)$$

The oligomer layer is liquidlike in all cases with the interaction energy between oligomer (o) monomers, $\varepsilon_{oo} = \varepsilon$. To model a liquid polymer (p) substrate, we take the interaction between monomers to be $\varepsilon_{pp} = \varepsilon$. Increasing ε_{pp} to 2.0ε allows us to study a glassy film, since the glass transition for long chain melts is $T_g \approx 0.5\varepsilon/k_B$.[38] For liquid polymer films, the interaction energy between polymer and oligomer monomers $\varepsilon_{po} = \varepsilon$, while for glassy polymer simulations $\varepsilon_{po} = 1.7\varepsilon$ or 2.0ε. For the glassy polymer, Berthelot's rule would give a mixing term of $\varepsilon_{po} = \sqrt{2}\varepsilon$. However, simulations with $\sqrt{2}\varepsilon$ or 1.5ε show little or no interdiffusion between the oligomer and polymer, though in both cases the oligomer and polymer films are completely wetting. Neighboring monomers in a chain interact through an additional FENE spring interaction,[39] with $k = 30\varepsilon$ and $R_0 = 1.5\sigma$. The bulk densities for the pure components of liquid polymers at $T = \varepsilon/k_B$ are $0.57\sigma^{-3}$ for monomers, $0.86\sigma^{-3}$ for $N = 10$, $0.88\sigma^{-3}$ for $N = 50$, and $0.89\sigma^{-3}$ for $N = 500$, while for $T = 0.5\varepsilon/k_B$, $\rho = 1.02\sigma^{-3}$ for $N = 500$. The entanglement length N_e is not known for this model since most previous studies have been for $r_c = 2^{1/6}\sigma$, $\rho = 0.85/\sigma^3$, and $T = \varepsilon/k_B$, for which $N_e \sim 70$.[39,40] N_e for the present case is expected to be somewhat less than 70 due to the slight increase in density.

Monomers in the polymer layer interact with a lower fixed featureless wall through a 9−3 Lennard-Jones potential[41] cutoff $r_c = 2.5\sigma$ with $\varepsilon_{wall} = 2.0\varepsilon$ for the liquidlike and 4.0ε for the glassy film. The interaction strength is chosen to prevent the polymer film from detaching from the lower wall. A purely repulsive 9−3 Lennard-Jones potential with a cutoff of $r_c = 0.71\sigma$ is used to confine the vapor phase of the upper layer. An upper wall is not needed for $N_o \geq 10$ since there are no chains in the vapor phase.

The equations of motion are integrated using a velocity-Verlet algorithm with a time step of $\Delta t = 0.01\tau$, where $\tau = \sigma(m/\varepsilon)^{1/2}$ and m is the monomer mass, identical for all monomers. The temperature of the system is held constant at $T = \varepsilon/k_B$ by a Langevin thermostat[39] ($\Gamma = 0.5\tau^{-1}$) acting only on the lowest 10σ of the film. Spatial confinement of the thermostat such that it is far from the interface minimizes any artificial dampening of long-range hydrodynamic interactions.[41] The oligomer and polymer films are constructed following the methodology discussed in Auhl et al.[42] An equilibration run of $20\,000\tau$ is performed for each before the two films are placed in contact.

Simulations were run for at least $80\,000\tau$ using the LAMMPS parallel molecular dynamics code.[43] The majority of the simulations were run on 512 to 1024 processors on Clemson's Palmetto cluster of Intel Xeon 2.33 GHz processors.[44] One million time steps ran for 9 h for the simulation with the largest number of monomers on 1024 processors.

III. Results

Figure 1 shows snapshots of the interfacial region for a liquid polymeric matrix for an entangled ($N_p = 500$) and an unentangled ($N_p = 50$) polymer in contact with an oligomer liquid of chain length $N_o = 10$ for different simulation times. Both polymer surfaces are relatively smooth at $t = 0$ and swell as interdiffusion of the oligomer proceeds. The unentangled polymer, $N_p = 50$, noticeably dissolves whereas the entangled

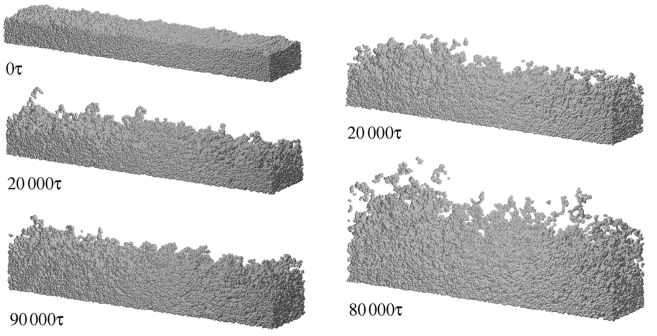

Figure 1. Snapshots of the interfacial region for a liquid polymer film for an entangled polymer of length $N_p = 500$ (left) and an unentangled polymer of length $N_p = 50$ (right) both in contact with a liquid of chain length $N_o = 10$ (not shown). The initial state for $N_p = 50$ is similar to that for $N_p = 500$. The base of the polymer film is at same height for all snapshots.

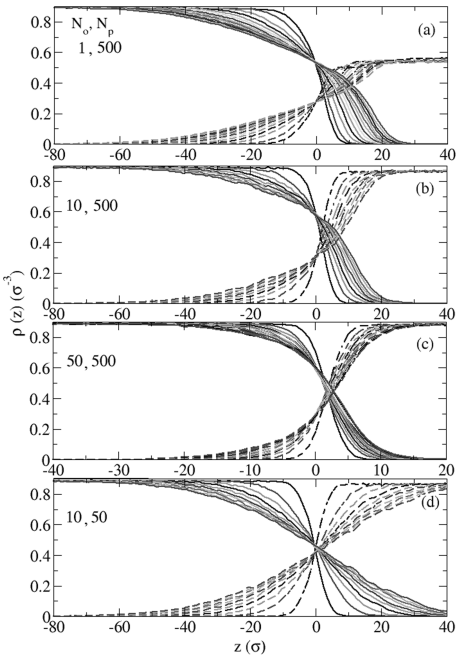

Figure 2. Density profiles $\rho(z)$ for oligomer (dashed) of chain length N_o on liquid polymer film of chain length N_p (solid). Results for (N_o, N_p): (a) (1, 500) $500\tau-13\,000\tau$, (b) (10, 500) $2000\tau-90\,000\tau$, (c) (50, 500) $2000\tau-136\,000\tau$, (d) (10, 50) $2000\tau-88\,000\tau$. All results for $\varepsilon_{po} = \varepsilon_{pp} = \varepsilon$.

polymer, $N_p = 500$, hardly dissolves by the latest time shown. The entangled polymer film forms a gel-like structure in this intermediate time regime.

Results for the time-dependent density profiles for an entangled polymer film of chain length $N_p = 500$ are shown in Figure 2 for a monomer ($N_o = 1$) and two short chain oligomers ($N_o = 10$, 50). Interdiffusion results in asymmetric density profiles at the interface between polymer-rich and oligomer-rich regions. The asymmetry is a result of different diffusion mechanisms in the two regions, which becomes more pronounced as the chain length of the oligomer increases. On the polymer-rich side of the interface, $z < 0$, scaling of z by $t^{-1/2}$ collapses each data set onto a single master curve as shown in Figure 3, consistent with a Fickian diffusion process for all cases studied. In the polymer-rich region, the system acts as a solvent penetrating an elastic solid, and the diffusivity as shown below is strongly dependent on the oligomer density. However, in the oligomer-rich region, the relatively slow process of polymer swelling and

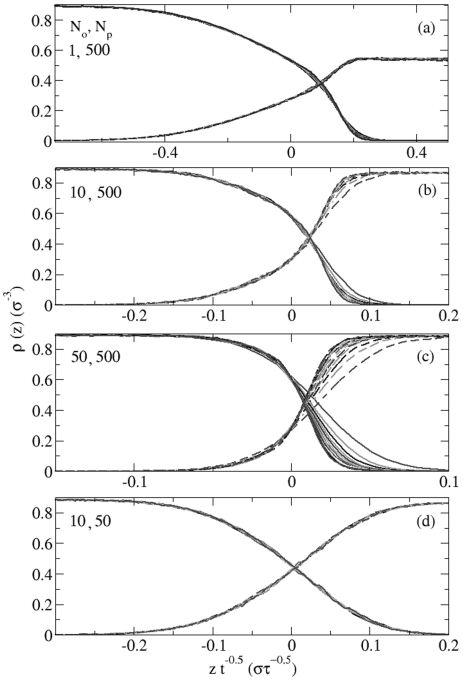

Figure 3. Density profiles $\rho(z)$ for oligomer of chain length N_o on liquid polymer film of chain length N_p versus scaled position $zt^{-1/2}$. Results for (N_o, N_p): (a) (1, 500), (b) (10, 500), (c) (50, 500), (d) (10, 50). The time range for each case is the same as in Figure 2.

disentanglement alters the interdiffusion process and the oligomer and polymer density profiles no longer scale with $\tau^{1/2}$ for $N \geq 10$. However, scaling z by $t^{-0.37}$ for $N_o = 10$ and $t^{-0.20}$ for $N_o = 50$ does collapse both the oligomer and polymer density profiles onto a single master curve. The polymer film changes from an elastic media to a responsive gel where the polymer has to rearrange to accommodate the larger solvent molecules as has been observed experimentally.[45]

For comparison, the interdiffusion of a short chain liquid of length $N_o = 10$ into a unentangled polymer matrix of chain length $N_p = 50$ is shown in Figure 2d. The density profiles for both the polymer and solvent on both sides of the interface are symmetric, in agreement with previous Monte Carlo simulations.[20,21] Scaling of z by $t^{-1/2}$ results in a master curve on both sides of the interface. In this case the polymer and solvent act at the interface as mixing of two simple liquids.

In order to investigate the role of the polymer interactions on the interdiffusion, we increased the interaction between monomers on the polymer chains to $\varepsilon_{pp} = 2\varepsilon$ so that the polymer film is near its glass transition temperature T_g.[38] For interactions between the oligomer and polymer which satisfy Berthelots mixing rule $\varepsilon_{po} = \sqrt{2}\varepsilon$ and for $\varepsilon_{po} = 1.5\varepsilon$ there is little or no interdiffusion between the oligomer and polymer, though the oligomer does completely wet the polymer film. However, for larger ε_{po} we do observe interdiffusion. The concentration profiles for two values of the interaction ε_{po} are shown in Figure 4. The profiles have a sharp convex shape, indicating a diffusive front. Scaling of z by $t^{-1/2}$ collapsed the data reasonably well onto a master curve for both $\varepsilon_{po} = 1.7\varepsilon$ and 2.0ε, indicating that the diffusion is Fickian in agreement with previous simulations of the interdiffusion of monomer solvents with glassy polymer films.[35]

The mass uptake of the solvent by the polymer film has been measured for all systems studied. Figure 5 shows the mass update in terms of the number of oligomer monomers that have diffused into the polymer as a function of $(t/\tau)^{1/2}$. For both liquid and glassy films, the mass uptake scales with $t^{1/2}$, consistent with Fickian interdiffusion in the polymer-rich region.

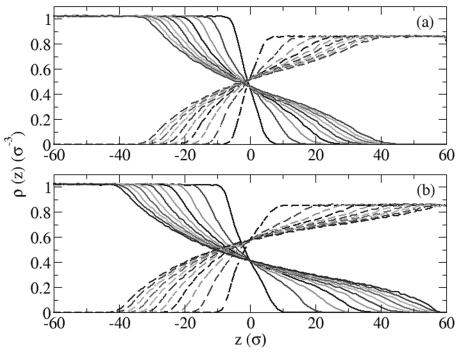

Figure 4. Density profiles for oligomer of length $N_o = 10$ (dashed) on glassy polymer (solid) of length $N_p = 500$. Results for (a) $\varepsilon_{po} = 1.7\varepsilon$ (2000τ–$90\,000\tau$), (b) $\varepsilon_{po} = 2.0\varepsilon$ (2000τ–$100\,000\tau$).

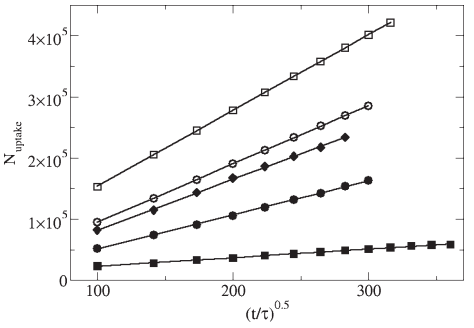

Figure 5. Mass uptake of oligomer by polymer versus $(t/\tau)^{1/2}$ for (N_o, N_p). Liquid polymer: (10, 500) (filled circle), (50, 500) (filled square), (10, 50) (filled diamond). Glassy polymer: (10, 500) $\varepsilon_{po} = 1.7\varepsilon$ (open circle) and $\varepsilon_{po} = 2\varepsilon$ (open square). Lines are least-squares fits.

Fick's second law has been used in conjunction with the density profiles to extract the density dependent diffusivity in the unswollen polymer-rich region

$$\frac{\partial \rho_s(z,t)}{\partial t} = \frac{\partial}{\partial z}\left[D(\rho_s(z,t))\frac{\partial \rho_s(z,t)}{\partial z}\right] \quad (2)$$

where $\rho_s(z,t)$ is the position- and time-dependent mass density of the diffusing species and $D(\rho_s(z,t))$ is the diffusivity. For Fickian diffusion, the diffusivity $D(\rho)$ is a function only of the concentration (density). As demonstrated by the mass uptake for all cases, diffusion is Fickian in the polymer-rich region. Additionally, the total density of the system is nearly constant in this region, varying by no more than 4% for any of the systems studied. Thus, $D(\rho)$ can be calculated in this regime for all cases. The swelling of the entangled polymer in the oligomer-rich region precludes Fickian diffusion;[46] thus, $D(\rho)$ cannot be calculated in this regime. This is evidenced by the lack of $t^{1/2}$ scaling of the density profiles in that region. For the ρ range corresponding to the polymer-rich region, eq 2 can be integrated through the use of a Boltzmann similarity transformation ($\eta = zt^{-1/2}$) to yield the concentration-dependent diffusivities[35,47]

$$D(\rho) = -\frac{1}{2}\left(\left.\frac{d\rho'}{d\eta}\right|_{\eta(\rho)}\right)^{-1}\int_{\eta_0}^{\eta}\eta'\frac{d\rho}{d\eta'}\,d\eta' \quad (3)$$

where η_0 refers to the scaled position at which the density becomes 0. Equation 3 has been used to calculate $D(\rho)$ from the scaled density profiles. Figure 6 displays the calculated $D(\rho)$ for values of ρ corresponding to the polymer-rich region. For $N_o = 10$ and $N_p = 50$, the diffusivity is nearly constant

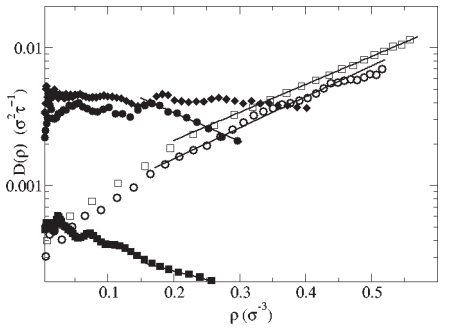

Figure 6. Concentration-dependent diffusivities $D(\rho)$ vs ρ. Results for (N_o, N_p): liquid polymer: (10, 500) (filled circle), (50, 500) (filled square), (10, 50) (filled diamond); glassy polymer: (10, 500) $\varepsilon_{po} = 1.7\varepsilon$ (open circle) and $\varepsilon_{po} = 2.0\varepsilon$ (open square). Lines are exponential fits.

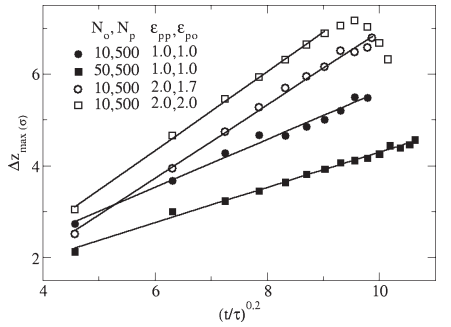

Figure 7. Roughness of the polymer surface Δz_{max} vs $(t/\tau)^{0.2}$. Results for (N_o, N_p): liquid polymer: (10, 500) (filled circle), (50, 500) (filled square); glassy polymer: (10, 500) $\varepsilon_{po} = 1.7\varepsilon$ (open circle) and $\varepsilon_{po} = 2\varepsilon$ (open square). Lines are least-squares fits.

across the entire concentration range, consistent with the mixing of the two simple liquids, where phenomena like entanglements and swelling do not occur. For the interdiffusion of oligomers of chain length $N_o = 10$ and 50 into an entangled polymer of length $N_p = 500$, the diffusivity of the oligomer is approximately constant for low concentration. At the higher concentrations, the diffusivity falls off exponentially, a signature of the hindrance of the diffusion brought on by polymer swelling as one crosses from the polymer-rich into the oligomer-rich region. The diffusion of $N_o = 10$ into the glassy polymer $N_p = 500$, $D(\rho)$ increases exponentially with concentration for both values of ε_{po} studied in agreement with predictions of the free-volume model.[48] Exponential diffusivities were also observed for the interdiffusion of monomers with glassy polymer films.[35]

As seen above, the swelling of the polymer film strongly affects the diffusion process. It also affects the roughness of the interface. The film roughness was measured by binning the monomers that comprise the polymer film in x–y grids of size 1σ. For each bin, the maximum height, z_{max}, of any monomer is found. The average of z_{max} over all x–y bins is determined, and the standard deviation is considered the roughness of the film. For the unentangled polymer film $N_o = 50$, the polymer chains dissolved, making the interface ill-defined. The roughness measurements were therefore carried out only for the entangled polymer film. The roughness of the swollen film was found to scale with $(t/\tau)^{0.2}$ as shown in Figure 7. While the roughness evolves as $t^{0.2}$ for all cases studied, except for the latest times for the glassy film with $\varepsilon_{po} = 2.0\varepsilon$, the origin of this power law is not yet understood. The roughness of the glassy film with $\varepsilon_{po} = 2.0\varepsilon$ deviates from the $(t/\tau)^{0.2}$ power law at $60\,000\tau$ and has a maximum roughness of approximately 7σ at $80\,000\tau$ before decreasing. This nonmonotonic trend is consistent with the evolving polymer film density profile as seen in Figure 4b. When the glassy film begins to swell

into the oligomer-rich region, some of the polymer chains start to disentangle from the film surface and extend into the oligomer film. These chains, as for the liquid film, are those that comprise the tail of the density profile and are the primary contributors to the surface roughness. Unlike the liquid film or the glassy film with $\varepsilon_{po} = 1.7\varepsilon$, for the glassy film with $\varepsilon_{po} = 2.0\varepsilon$, a convex diffusion front grows into the oligomer-rich region at a faster rate than this tail, causing the tail to shrink significantly and nearly vanish by the latest time of $100\,000\tau$. The loss of this tail is responsible for the decreasing surface roughness as the density profile becomes more convex.

IV. Summary

The crossover from a simple liquid to a short oligomer diffusing into liquid and glassy entangled polymer matrices has been studied by molecular dynamics simulations. As the oligomer penetrates the polymer, two distinct regions form at the interface: an unswollen polymer-rich region with a low oligomer concentration and a gel-like oligomer-rich region into which the polymer has begun to swell. Each region displays distinct diffusive dynamics which become more pronounced as the chain length of the oligomer increases. In the polymer-rich region, for both liquid and glassy matrices, the mass uptake of the oligomer and the density profiles for both oligomer and polymer scale as $t^{1/2}$, characteristic of Fickian interdiffusion. For the liquid polymer matrix, this region is essentially composed of a mixture of viscous fluids that obey classical Fickian diffusion. For glassy polymer matrix, the oligomer diffuses into an elastic solid, which again can be described by a Fickian diffusion process in the polymer-rich region. In the swollen oligomer-rich region for both liquid and glassy matrices, the diffusion diverges from the classical Fickian process, though still following a power law. The scaling exponent depends on the nature of the polymer, the chain length of the oligomer and the polymer, and the strength of the interaction. This behavior differs significantly from the interpenetration of two short oligomers, in which case Fickian interdiffusion is observed on both sides of the interface. For the oligomers penetrating into an entangled, liquid film, $D(\rho)$ is constant at low oligomer concentration and decreases exponentially as concentration increases. Diffusion of oligomers into a glassy film exhibits an exponential increase with oligomer concentration due to the strong polymer/oligomer interaction ε_{op}.

This study resolved the differences between the diffusion of unentangled oligomers into polymeric matrices from that of simple liquids. Clear distinctions are observed even for very short oligomers. This study provides a first step toward understanding the interdiffusion of larger species in polymeric materials.

Acknowledgment. We thank the DOE for partial support of this work under Contract No. ER46456. This work was performed, in part, at the Center for Integrated Nanotechnologies, a U.S. Department of Energy, Office of Basic Energy Sciences user facility. Sandia is a multiprogram laboratory operated by Sandia Corporation, a Lockheed Martin Company, for the United States Department of Energy under Contract No. DE-AC04-94AL85000. This work was made possible by advanced computational resources deployed and maintained by Clemson Computing and Information Technology.

References and Notes

(1) Morton-Jones, D. H.; Ellis, J. W. *Polymer Products: Design, Materials, and Processing*; Chapman and Hall: London, England, 1986.
(2) Wool, R. P. *Polymer Interfaces: Structure and Strength*; Hanser Publishers: Munich, Germany, 1995.
(3) Stamm, M., Ed. *Polymer Surfaces and Interfaces: Characterization, Modification and Applications*; Springer: Berlin, 2008.
(4) Youngblood, J. P.; Sottos, N. R. *MRS Bull.* **2008**, *33*, 732.
(5) Kramer, E. J.; Green, P.; Palmstrom, C. J. *J. Chem. Phys.* **1984**, *25*, 473.
(6) Composto, R. J.; Kramer, E. J.; White, D. M. *Nature* **1987**, *328*, 234.
(7) Chaturvedi, U. K.; Steiner, U.; Zak, O.; Krausch, G.; Klein, J. *Phys. Rev. Lett.* **1989**, *63*, 616.
(8) Kausch, H. H.; Tirrell, M. *Annu. Rev. Mater. Sci.* **1989**, *19*, 341.
(9) Steiner, U.; Chaturvedi, U. K.; Zak, O.; Schatz, G.; Klein, J. *Macromol. Liq.* **1990**, *177*, 367.
(10) Reiter, G.; Hüttenbach, S.; Foster, M.; Stamm, M. *Macromolecules* **1991**, *24*, 1179.
(11) Welp, K. A.; Wool, R. P.; Satija, S. K.; Pispas, S.; Mays, J. *Macromolecules* **1998**, *31*, 4915.
(12) Welp, K. A.; Wool, R. P.; Agrawal, G.; Satija, S. K.; Pispas, S.; Mays, J. *Macromolecules* **1999**, *32*, 5127.
(13) Bucknall, D. G.; Higgins, J. S.; Butler, S. A. *Chem. Eng. Sci.* **2001**, *56*, 5473.
(14) Kwan, K. S.; Subramaniamb, C. N. P.; Ward, T. C. *Polymer* **2003**, *44*, 3061.
(15) Kwan, K. S.; Subramaniamb, C. N. P.; Ward, T. C. *Polymer* **2003**, *44*, 3071.
(16) Perahia, D.; Llin, H.; Majewski, J.; Smith, H.; Cornelius, C.; Fujimoto, C. *Macromolecules*, in press.
(17) Brochard-Wyart, F. *Kinetics of Polymer/Polymer Interdiffusion*; Elsevier: New York, 1988; pp 249−256.
(18) Zhang, H.; Wool, R. P. *Macromolecules* **1989**, *22*, 3018.
(19) Brochard-Wyart, F.; de Gennes, P. G. *Makromol. Chem.* **1990**, *40*, 167.
(20) Jilge, W.; Carmesin, I.; Kremer, K.; Binder, K. *Macromolecules* **1990**, *23*, 5001.
(21) Deutsch, H. P.; Binder, K. *J. Chem. Phys.* **1991**, *94*, 2294.
(22) Haire, K. R.; Windle, A. H. *Comput. Theor. Polym. Sci.* **2001**, *11*, 227.
(23) Anderson, K. L.; Wescott, A. H. W. J. T.; Carver, T. J. *Mater. Sci. Eng., A* **2004**, *A365*, 14.
(24) Sanopoulou, M.; Stamatialis, D. *Polymer* **2001**, *42*, 1429.
(25) Greenfield, M. L.; Theodorou, D. N. *Macromolecules* **2001**, *34*, 8541.
(26) Argon, A. S.; Cohen, R. E.; Patel, A. C. *Polymer* **1999**, *40*, 6991.
(27) Thomas, N. L.; Windle, A. H. *Polymer* **1981**, *22*, 627.
(28) Alfrey, T.; Gurnee, E. F.; Lloyd, W. G. *J. Polym. Sci.* **1966**, *C12*, 249.
(29) Hassan, M. M.; Durning, C. J. *J. Polym. Sci., Part A* **1999**, *37*, 3159.
(30) Stamatialis, M.; Sanopoulous, M.; Petropoulos, J. H. *Macromolecules* **2002**, *35*, 1021.
(31) Durning, C. J.; Hassan, M. M.; Tong, H. M.; Lee, K. W. *Macromolecules* **1995**, *28*, 4234.
(32) Condamin, S.; Tejedor, V.; Voituriez, R.; nichou, O. B.; Klafter, J. *Proc. Natl. Acad. Sci. U.S.A.* **2008**, *105*, 5675.
(33) Saxton, M. J. *Biophys. J.* **1994**, *66*, 394.
(34) Wong, I.; Gardel, M. L.; Reichman, D. R.; Weeks, E. R.; Valentine, M. T.; Bausch, A. R.; Weitz, D. A. *Phys. Rev. Lett.* **2004**, *92*, 178101.
(35) Tsige, M.; Grest, G. S. *J. Chem. Phys.* **2004**, *121*, 7513.
(36) Tsige, M.; Grest, G. S. *J. Chem. Phys.* **2004**, *120*, 2989.
(37) von Meerwall, E.; Skowronski, D.; Hariharan, A. *Macromolecules* **1991**, *24*, 2441.
(38) Baljon, A. R. C.; Robbins, M. O. *Macromolecules* **2001**, *34*, 4200.
(39) Kremer, K.; Grest, G. S. *J. Chem. Phys.* **1990**, *92*, 5057.
(40) Everaers, R.; Sukumaran, S. K.; Grest, G. S.; Svaneborg, C.; Sivasubramanian, A.; Kremer, K. *Science* **2004**, *303*, 823.
(41) Heine, D. R.; Grest, G. S.; Webb, E. B.III *Phys. Rev. E* **2003**, *68*, 061603. *Phys. Rev. E* **2004**, *70*, 011606.
(42) Auhl, R.; Everaers, R.; Grest, G. S.; Kremer, K.; Plimpton, S. J. *J. Chem. Phys.* **2003**, *119*, 12718.
(43) Plimpton, S. J. *J. Comput. Phys.* **1995**, *117*, 1.
(44) The Clemson Palmetto cluster is composed of 512 Dell PowerEdge 1950 Intel Xeon E5345 2.33 GHz and 260 SunFire X2200 AMD Opteron 2.3 GHz nodes.
(45) Vrentas, J. S.; Duda, J. L.; Huang, W. J. *Macromolecules* **1986**, *19*, 1718.
(46) Kuipers, N. J. M.; Beenackers, A. A. C. M. *Chem. Eng. Sci.* **1993**, *48*, 2957.
(47) Crank, J. *The Mathematics of Diffusion*; Oxford University Press: Oxford, 1975.
(48) Korsmeyere, R. W.; von Meerwall, E.; Peppas, N. A. *J. Polym. Sci.* **1986**, *24*, 409.